

Plane-wave scattering by a perfectly conducting circular cylinder near a plane surface: cylindrical-wave approach

R. Borghi, F. Gori, and M. Santarsiero

Dipartimento di Fisica, Università La Sapienza, Piazzale Aldo Moro 2, 00185 Rome, Italy

F. Frezza and G. Schettini

Dipartimento di Ingegneria Elettronica, Università La Sapienza, Via Eudossiana 18, 00184 Rome, Italy

Received January 3, 1995; revised manuscript received September 15, 1995; accepted September 20, 1995

A new method for the analysis of the diffraction of a plane wave impinging on a perfectly conducting circular cylinder in front of a generally reflecting surface is presented. The surface is characterized by its complex reflection coefficient, enabling us to treat a wide class of reflecting surfaces. The presence of the surface is taken into account by means of a suitable expansion of the reflected field in terms of cylindrical functions. The method gives the solution of the scattering problem in both the near and the far field regardless of the polarization state of the incident field. Numerical examples for dielectric interfaces are presented, and comparisons are made with results presented in the literature. © 1996 Optical Society of America

1. INTRODUCTION

Plane-wave scattering by a perfectly conducting circular cylinder in an isotropic and homogeneous medium is a classical problem, whose solution can be found in several books of fundamental electromagnetism.^{1,2} Moreover, the case of an arbitrary-cross-section cylinder has been treated by numerical methods.³⁻⁷

If the cylinder is placed near a plane of discontinuity for the electromagnetic constants, the scattering problem assumes a more complicated form. If the surface of discontinuity is a perfectly conducting mirror, it is possible to use image methods,⁸⁻¹¹ and the problem is reduced to that of several cylinders in a homogeneous medium.¹²⁻¹⁴ The case of a conducting surface of finite extent has also been treated.¹⁵⁻¹⁷ For the case in which the surface is a dielectric interface or a real conducting substrate, solutions have been presented for the far field^{18,19} and also for noncylindrical objects.²⁰⁻²⁷

In the limit of very small (with respect to the wavelength) radii, the cylinders reduce to wires and the problem can be solved by use of effective-impedance methods.^{28,29} For circular conducting cylinders of arbitrary size in the presence of interfaces with arbitrary reflection properties, the problem has not yet been solved in a general and rigorous way.

The method presented here gives the determination of the field diffracted by a perfectly conducting cylinder placed near a plane surface with a given reflection coefficient Γ , which is an arbitrary function of the incidence angle, when the structure is illuminated by a plane wave. The formulation allows us to treat both the far and the near field for both TM and TE polarization and can be applied also to interfaces between an isotropic and an anisotropic medium, such as a thermonuclear plasma.³⁰

The study of this class of problems is useful in a

wide variety of applications. For instance, we may recall the propagation and diffraction of microwave beams by arrays of scattering elements,³¹ the radar detection of objects near the ground,¹⁸ the design of diffractive optical gratings,³² and the study of quasi-optical launchers of lower-hybrid plasma waves,³⁰ for which a highly accurate evaluation of the near field is necessary. These techniques are of interest also for the study of surface contamination in the semiconductor industry.³³

The theoretical analysis of the problem is presented in Section 2, where procedures for the evaluation of the electromagnetic field are developed. In Section 3 some numerical results regarding the case of a dielectric interface are reported for the near-field distribution for both polarization states. Furthermore, comparisons are made in some particular cases with different approaches for the far-field patterns, with very good agreement. Possible extensions of the present theory are discussed in Section 4.

2. THEORETICAL ANALYSIS

The method described here gives a rigorous analysis of plane-wave scattering by a perfectly conducting circular cylinder close to a nonideal mirror, i.e., a plane interface characterized by an angle-dependent reflection coefficient.

To obtain the solution without any mirror, i.e., in an isotropic and homogeneous medium, it is customary to express the total field as the sum of two terms: the incident plane wave and a diffracted field. The latter can be expanded in terms of cylindrical functions, which are defined as the product of a Hankel function of the first kind of integer order $H_n^{(1)}$ times a sinusoidal angular factor $\exp(in\vartheta)$. The time dependence of the field is assumed to be $\exp(-i\omega t)$, where ω is the angular frequency. One can determine the complex expansion coefficients by im-

posing the electromagnetic boundary conditions on the surface of the conducting cylinder.¹

In the case of an ideal mirror the total field can be expressed as the sum of the incident plane wave, a diffracted field, and two further terms that are produced by the reflection of the incident plane wave and the diffracted wave, respectively. The last term will be denoted the diffracted–reflected field. This is equivalent to the use of the image method.^{8–11}

Dealing with a nonideal mirror, we preserve the ideal-mirror scheme, using the four terms just indicated. The main difficulties arise from the diffracted–reflected field. In fact, as we said above, the diffracted field is easily expressed in terms of cylindrical outgoing waves, but the reflection properties of a plane of discontinuity are known only for plane incident waves.¹

The key to solving this problem is the use of the analytical plane-wave spectrum of the cylindrical waves.³⁴ In this way we may characterize the surface by means of only its plane-wave reflection coefficient, which can be an arbitrary function of the generally complex wave vector. As a consequence, we can deal with rather general interfaces, such as those with anisotropic media, multilayered media, and lossy media. A quite similar approach has been adopted with reference to spherical waves.²⁰

In Fig. 1 the geometrical layout of the problem is shown. The axis of the cylinder is parallel to the *y* axis and is at a distance *h* from the interface. The structure is assumed to be infinite along the *y* direction, so that the problem is reduced to a two-dimensional form. The wave vector of the incident field, **k**^{*i*}, lies in the *x*–*z* plane. The polarization is said to be TM (with respect to the axis of the cylinder) or *E* when the electric field is directed along the *y* axis, and TE or *H* when the magnetic field is axially directed. φ is the angle between **k**^{*i*} and the *x* axis, and ψ specifies the propagation direction of a typical plane wave building up the angular spectrum of the field diffracted by the cylinder. For the sake of brevity the following dimensionless notation is used: $\xi = kx$, $\zeta = kz$, and $\chi = kh$, where *k* is the wave number. A polar coordinate system (ρ, ϑ), with $\rho = kr$, centered on the cylinder axis has been introduced. In the following, $V(\xi, \zeta)$ stands for the component of the electromagnetic field parallel to the *y* axis; i.e., $V = E_y$ for TM polarization and $V = H_y$ for TE polarization.

The incident field wave vector **k**^{*i*} is related to the angle φ through the following expressions:

$$\begin{aligned} k_{\parallel}^i &= k \sin \varphi, \\ k_{\perp}^i &= k \cos \varphi, \end{aligned} \tag{1}$$

where the symbols \perp and \parallel refer to the orthogonal and the parallel components, respectively, of a vector with respect to the interface. The presence of the interface is described by the complex reflection coefficient $\Gamma(n_{\parallel})$, where $\mathbf{n} = \mathbf{k}/k$ is the unit vector parallel to **k**.

According to the above-outlined procedure, the total field is expressed as the superposition of the following four fields:

- V_i , field of the incident plane wave;
- V_r , field due to the reflection of V_i by the plane surface;

- V_d , field diffracted by the cylinder;
- V_{dr} , field due to the reflection of V_d by the plane surface.

In applying the boundary conditions on the circular cylinder it is useful to express the aforementioned fields in terms of functions that have cylindrical symmetry, centered on the axis of the cylinder itself. By use of the expansion of a plane wave in terms of Bessel functions $J_l(x)$, the incident field V_i may be expressed as

$$\begin{aligned} V_i(\xi, \zeta) &= V_0 \exp(in_{\perp}^i \xi + in_{\parallel}^i \zeta) \\ &= V_0 \sum_{l=-\infty}^{+\infty} i^l \exp(-il\varphi) J_l(\rho) \exp(il\vartheta). \end{aligned} \tag{2}$$

The field V_d is expressed as the sum of the following cylindrical functions CW_l , defined as

$$CW_l(\xi, \zeta) = H_l^{(1)}(\rho) \exp(il\vartheta), \tag{3}$$

with unknown coefficients c_l ; of course, the (ξ, ζ) dependence is implicit in ρ and ϑ . Hence we have

$$V_d(\xi, \zeta) = V_0 \sum_{l=-\infty}^{+\infty} i^l \exp(-il\varphi) c_l CW_l(\xi, \zeta), \tag{4}$$

where the term $i^l \exp(-il\varphi)$ has been added to make the comparison with Eq. (2) easier. The reflected field V_r is given by

$$\begin{aligned} V_r(\xi, \zeta) &= V_0 \Gamma(n_{\parallel}^i) \exp(in_{\perp}^i 2\chi - in_{\perp}^i \xi + in_{\parallel}^i \zeta) \\ &= V_0 \Gamma(n_{\parallel}^i) \exp(in_{\perp}^i 2\chi) \sum_{l=-\infty}^{+\infty} i^l J_l(\rho) \exp[il(\vartheta - \varphi')], \end{aligned} \tag{5}$$

where $\varphi' = \pi - \varphi$ denotes the angle of propagation of the reflected wave.

As discussed in Appendix A, the V_{dr} field is given by

$$V_{dr}(\xi, \zeta) = V_d(2\chi - \xi, \zeta) * \hat{\Gamma}(\zeta), \tag{6}$$

where the asterisk denotes convolution with respect to

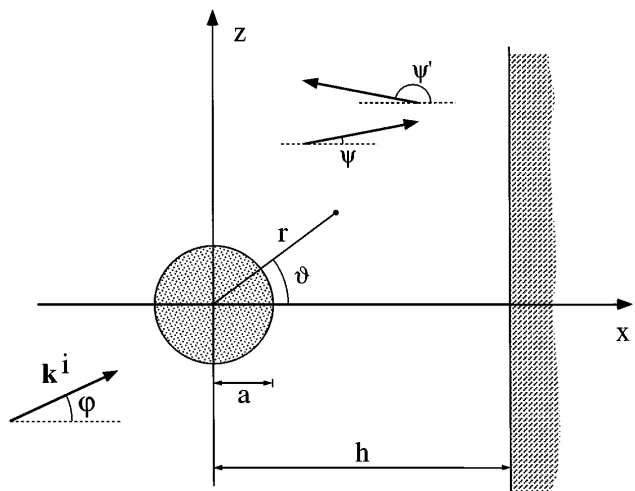


Fig. 1. Geometry of the problem and notation used throughout the paper.

the ζ variable, and $\hat{\Gamma}(\zeta)$ represents the inverse Fourier transform of the reflection coefficient; i.e.,

$$\hat{\Gamma}(\zeta) = \frac{1}{2\pi} \int_{-\infty}^{+\infty} \Gamma(n_{\parallel}) \exp(in_{\parallel}\zeta) dn_{\parallel}. \quad (7)$$

Then, recalling Eqs. (4) and (6), we have

$$\begin{aligned} V_{dr}(\xi, \zeta) &= V_0 \sum_{l=-\infty}^{+\infty} i^l \exp(-il\varphi) c_l CW_l(2\chi - \xi, \zeta) * \hat{\Gamma}(\zeta) \\ &= V_0 \sum_{l=-\infty}^{+\infty} i^l \exp(-il\varphi) c_l RW_l(2\chi - \xi, \zeta), \end{aligned} \quad (8)$$

where the functions $RW_l(\xi, \zeta) = CW_l(\xi, \zeta) * \hat{\Gamma}(\zeta)$ take on an explicit form if we introduce the angular spectrum of cylindrical functions with respect to the variable ζ . Such a spectrum, denoted by $F_l(\xi, n_{\parallel})$, is related to the CW_l functions by

$$CW_l(\xi, \zeta) = \frac{1}{2\pi} \int_{-\infty}^{+\infty} F_l(\xi, n_{\parallel}) \exp(in_{\parallel}\zeta) dn_{\parallel}. \quad (9)$$

With use of this equation, the $RW_l(\xi, \zeta)$ functions become

$$RW_l(\xi, \zeta) = \frac{1}{2\pi} \int_{-\infty}^{+\infty} \Gamma(n_{\parallel}) F_l(\xi, n_{\parallel}) \exp(in_{\parallel}\zeta) dn_{\parallel}. \quad (10)$$

The explicit expression of the functions $F_l(\xi, n_{\parallel})$ is given in Ref. 34 and after some algebra can be rewritten, for both homogeneous and evanescent waves, as (see Appendix B)

$$F_l(\xi, n_{\parallel}) = \frac{2 \exp(in_{\perp}\xi)}{n_{\perp}} \exp(-il \arccos n_{\parallel}), \quad (11)$$

where $n_{\perp} = \sqrt{1 - n_{\parallel}^2}$ and the function \arccos is meant to be defined over the whole real axis.

From Eqs. (8) and (10), taking into account that a shift in the ξ variable corresponds to a multiplication by an exponential factor [see Eq. (11)], we have the following expression:

$$\begin{aligned} V_{dr}(\xi, \zeta) &= V_0 \sum_{l=-\infty}^{+\infty} i^l \exp(-il\varphi) c_l \frac{1}{2\pi} \int_{-\infty}^{+\infty} \Gamma(n_{\parallel}) F_l(2\chi, n_{\parallel}) \\ &\quad \times \exp(-in_{\perp}\xi + in_{\parallel}\zeta) dn_{\parallel}. \end{aligned} \quad (12)$$

By expressing the plane wave in the integral in Eq. (12) through a series as in Eq. (2), we have

$$\begin{aligned} V_{dr}(\xi, \zeta) &= V_0 \sum_{l=-\infty}^{+\infty} i^l \exp(-il\varphi) c_l \sum_{m=-\infty}^{+\infty} i^m J_m(\rho) \\ &\quad \times \exp[im(\vartheta - \psi')] \\ &\quad \times \frac{1}{2\pi} \int_{-\infty}^{+\infty} \Gamma(n_{\parallel}) F_l(2\chi, n_{\parallel}) dn_{\parallel}, \end{aligned} \quad (13)$$

where (see Fig. 1) $\psi' = \pi - \psi$, the angle ψ being defined as $\psi = \arcsin n_{\parallel}$. Rearranging Eq. (13), we have

$$\begin{aligned} V_{dr}(\xi, \zeta) &= V_0 \sum_{l=-\infty}^{+\infty} i^l \exp(-il\varphi) c_l \sum_{m=-\infty}^{+\infty} i^m J_m(\rho) (-1)^m \exp(im\vartheta) \\ &\quad \times \frac{1}{2\pi} \int_{-\infty}^{+\infty} \Gamma(n_{\parallel}) \frac{2 \exp(in_{\perp}2\chi)}{n_{\perp}} \exp(-il \arccos n_{\parallel}) \\ &\quad \times \exp(im \arcsin n_{\parallel}) dn_{\parallel} \\ &= V_0 \sum_{l=-\infty}^{+\infty} i^l \exp(-il\varphi) c_l \sum_{m=-\infty}^{+\infty} J_m(\rho) \exp(im\vartheta) \\ &\quad \times \frac{1}{2\pi} \int_{-\infty}^{+\infty} \Gamma(n_{\parallel}) \frac{2 \exp(in_{\perp}2\chi)}{n_{\perp}} \\ &\quad \times \exp[-i(l+m) \arccos n_{\parallel}] dn_{\parallel}, \end{aligned} \quad (14)$$

where the trigonometric relation

$$\exp(im \arcsin n_{\parallel}) = i^m \exp(-im \arccos n_{\parallel}) \quad (15)$$

is used. Thus we obtain

$$\begin{aligned} V_{dr}(\xi, \zeta) &= V_0 \sum_{l=-\infty}^{+\infty} i^l \exp(-il\varphi) c_l \sum_{m=-\infty}^{+\infty} J_m(\rho) \exp(im\vartheta) \\ &\quad \times \frac{1}{2\pi} \int_{-\infty}^{+\infty} \Gamma(n_{\parallel}) F_{l+m}(2\chi, n_{\parallel}) dn_{\parallel} \\ &= V_0 \sum_{l=-\infty}^{+\infty} i^l \exp(-il\varphi) c_l \sum_{m=-\infty}^{+\infty} J_m(\rho) \\ &\quad \times \exp(im\vartheta) RW_{l+m}(2\chi, 0). \end{aligned} \quad (16)$$

Once the expressions of all fields in the frame centered on the cylinder axis are given, we have to impose the boundary conditions on the surface of the cylinder, namely

$$\begin{aligned} [V_i + V_r + V_d + V_{dr}]_{\rho=ka} &= 0 \quad \text{for TM polarization,} \\ [V_i + V_r + V_d + V_{dr}]'_{\rho=ka} &= 0 \quad \text{for TE polarization,} \end{aligned} \quad (17)$$

where the prime denotes derivation with respect to the variable ρ . By using Eqs. (2), (4), (5), (16), and (17), after some algebra we obtain the following linear system for the unknown coefficients c_l :

$$\sum_{l=-\infty}^{+\infty} A_{ml} c_l = b_m, \quad (18)$$

where

$$\begin{aligned} A_{ml} &= \exp(-il\varphi) [\delta_{ml} + i^{l-m} G_m(ka) RW_{l+m}(2\chi, 0)], \\ b_m &= -G_m(ka) \{ \exp(-im\varphi) + \Gamma(n_{\parallel}^i) \exp(i2n_{\perp}^i \chi) \\ &\quad \times \exp[-im(\pi - \varphi)] \}, \end{aligned} \quad (19)$$

and the symbol δ_{ml} denotes the Kronecker delta. The function G_m , which contains the information regarding the boundary conditions, is defined as follows:

$$G_m(x) = \begin{cases} \frac{J_m(x)}{H_m^{(1)}(x)} & \text{for TM polarization} \\ \frac{J'_m(x)}{H_m^{(1)'}(x)} & \text{for TE polarization} \end{cases} \quad (21)$$

It is useful to note that, if Γ is constant with respect to n_{\parallel} , the integral in Eq. (16) can be performed analytically and the V_{dr} field reduces to the field diffracted by an image cylinder, placed in $\xi = 2\chi$, under the action of V_r as the incident field. Moreover if $\Gamma = 0$, i.e., in absence of the interface, Eqs. (5) and (6) show that $V_r = 0$ and $V_{dr} = 0$, so that linear system (18) yields the classical solution for scattering in an isotropic and homogeneous medium.¹

Once system (18) has been solved, it is possible to evaluate the electric (magnetic) field for TM (TE) polarization by means of Eqs. (2), (4), (5), and (16). For complete information on the electromagnetic field to be obtained, the magnetic (electric) field for TM (TE) polarization remains to be evaluated.

From Maxwell's equations we obtain

$$\begin{aligned} \mathbf{E} &= \frac{i}{\omega\epsilon} \nabla \times \mathbf{H}, \\ \mathbf{H} &= -\frac{i}{\omega\mu} \nabla \times \mathbf{E}. \end{aligned} \quad (22)$$

By using dimensionless coordinates, we have

$$\nabla = k\tilde{\nabla}, \quad (23)$$

where the symbol $\tilde{\nabla}$ denotes the gradient with respect to the dimensionless coordinates. By substituting Eq. (23) into Eq. (22), we obtain

$$\begin{aligned} \mathbf{E}(\rho) &= \frac{ik}{\omega\epsilon} \tilde{\nabla} \times \mathbf{H}(\rho) = iZ\tilde{\nabla} \times \mathbf{H}(\rho), \\ \mathbf{H}(\rho) &= -\frac{ik}{\omega\mu} \tilde{\nabla} \times \mathbf{E}(\rho) = \frac{1}{iZ} \tilde{\nabla} \times \mathbf{E}(\rho), \end{aligned} \quad (24)$$

where $Z = \sqrt{\mu/\epsilon}$.

Regardless of the polarization state of the incident field, one has to evaluate the curl of $V(\xi, \zeta)\hat{\mathbf{y}}$, where the symbol $\hat{\mathbf{y}}$ denotes a unit vector, i.e.,

$$\tilde{\nabla} \times V(\xi, \zeta)\hat{\mathbf{y}} = -\partial_{\zeta}V(\xi, \zeta)\hat{\mathbf{x}} + \partial_{\xi}V(\xi, \zeta)\hat{\mathbf{z}}. \quad (25)$$

Thus we can write, for TM polarization,

$$\begin{aligned} \mathbf{E}(\xi, \zeta) &= V(\xi, \zeta)\hat{\mathbf{y}}, \\ \mathbf{H}(\xi, \zeta) &= -\frac{1}{iZ} \partial_{\zeta}V(\xi, \zeta)\hat{\mathbf{x}} + \frac{1}{iZ} \partial_{\xi}V(\xi, \zeta)\hat{\mathbf{z}}, \end{aligned} \quad (26)$$

and, for TE polarization,

$$\begin{aligned} \mathbf{E}(\xi, \zeta) &= -iZ\partial_{\zeta}V(\xi, \zeta)\hat{\mathbf{x}} + iZ\partial_{\xi}V(\xi, \zeta)\hat{\mathbf{z}}, \\ \mathbf{H}(\xi, \zeta) &= V(\xi, \zeta)\hat{\mathbf{y}}. \end{aligned} \quad (27)$$

As a consequence, to evaluate the total field, one has to use the partial derivatives of $V(\xi, \zeta)$, and in particular the partial derivatives of $CW_l(\xi, \zeta)$ and $RW_l(\xi, \zeta)$ [see Eqs. (4) and (8)]. The detailed analysis, carried out in Appendix C, yields

$$\partial_{\xi}CW_l(\xi, \zeta) = 1/2[CW_{l-1}(\xi, \zeta) - CW_{l+1}(\xi, \zeta)], \quad (28)$$

$$\partial_{\zeta}CW_l(\xi, \zeta) = i/2[CW_{l-1}(\xi, \zeta) + CW_{l+1}(\xi, \zeta)], \quad (29)$$

$$\partial_{\xi}RW_l(\xi, \zeta) = 1/2[RW_{l-1}(\xi, \zeta) - RW_{l+1}(\xi, \zeta)], \quad (30)$$

$$\partial_{\zeta}RW_l(\xi, \zeta) = i/2[RW_{l-1}(\xi, \zeta) + RW_{l+1}(\xi, \zeta)]. \quad (31)$$

Through the knowledge of these functions, the evaluation of the transverse component of the electromagnetic field may be carried out in a straightforward way.

Once system (18) has been solved, it is possible to evaluate the total electromagnetic field for both polarization states, through only the knowledge of the scalar function $V(\xi, \zeta)$. In particular, the total diffracted field $V_d^{\text{tot}} = V_d + V_{dr}$ is given by

$$\begin{aligned} V_d^{\text{tot}}(\xi, \zeta) &= V_0 \left[\sum_{l=-\infty}^{+\infty} \hat{c}_l CW_l(\xi, \zeta) + \sum_{l=-\infty}^{+\infty} \hat{c}_l RW_l(2\chi - \xi, \zeta) \right] \\ &= V_0 \sum_{l=-\infty}^{+\infty} \hat{c}_l [CW_l(\xi, \zeta) + RW_l(2\chi - \xi, \zeta)], \end{aligned} \quad (32)$$

where, for the sake of simplicity, we put $\hat{c}_l = i^l \exp(-il\varphi)c_l$. The diffracted field in the far zone is easily calculated by use of the asymptotic expansion of the Hankel function³⁵:

$$H_l^{(1)}(\rho) \approx \sqrt{-2i/\pi\rho} i^{-l} \exp(i\rho). \quad (33)$$

In fact, for the CW_l , we obtain the following far-field expression:

$$CW_l(\xi, \zeta) \approx \sqrt{-2i/\pi\rho} i^{-l} \exp(i\rho + il\vartheta), \quad (34)$$

of which the coordinates (ρ, ϑ) are shown in Fig. 2. With respect to the functions RW_l , the following expression is obtainable^{36,37}:

$$RW_l(\xi, \zeta) \approx \sqrt{-2i/\pi\rho} \Gamma(\sin \vartheta) i^{-l} \exp(i\rho + il\vartheta), \quad (35)$$

corresponding to the well-known interpretation of the far field by means of plane waves. Therefore

$$RW_l(2\chi - \xi, \zeta) \approx \sqrt{-2i/\pi\bar{\rho}} \Gamma(\sin \bar{\vartheta}) i^{-l} \exp(i\bar{\rho} + il\bar{\vartheta}), \quad (36)$$

where $(\bar{\rho}, \bar{\vartheta})$ are also shown in Fig. 2.

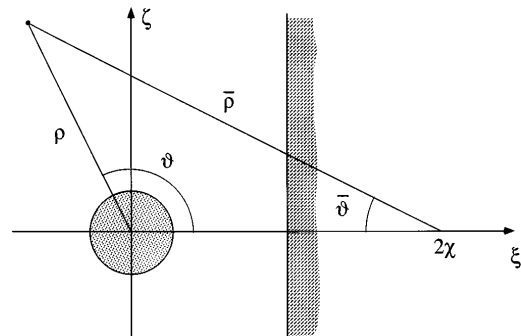


Fig. 2. Notation used in Section 2.

To compute the far field, we can substitute from relations (34) and (36) into Eq. (32), making the following approximations:

$$\begin{aligned} \frac{1}{\bar{\rho}} &\approx \frac{1}{\rho}, \\ \bar{\vartheta} &\approx \pi - \vartheta, \\ \exp(i\bar{\rho}) &\approx \exp(-2i\chi \cos \vartheta)\exp(i\rho). \end{aligned} \quad (37)$$

After some algebra we finally obtain the far-field expression of the total diffracted field:

$$\begin{aligned} V_d^{\text{tot}}(\xi, \zeta) &\approx V_0 \sqrt{-2i/\pi\rho} \exp(i\rho) \sum_{l=-\infty}^{+\infty} i^{-l} \hat{c}_l \\ &\times [\exp(il\vartheta) + (-1)^l \Gamma(\sin \vartheta) \\ &\times \exp(-2i\chi \cos \vartheta)\exp(-il\vartheta)]. \end{aligned} \quad (38)$$

The far-field pattern can be thought of as the angular part of relation (38); i.e.,

$$\begin{aligned} g(\vartheta) &\approx \sum_{l=-\infty}^{+\infty} i^{-l} \hat{c}_l [\exp(il\vartheta) + (-1)^l \Gamma(\sin \vartheta) \\ &\times \exp(-2i\chi \cos \vartheta)\exp(-il\vartheta)]. \end{aligned} \quad (39)$$

In the particular case of a thin wire above a plane interface, Eq. (39) reduces to the result given in Ref. 38 for TM polarization, since only the Hankel function of zero order is significant. On the other hand, in the TE case, as is well known, the first higher-order terms ($l \pm 1$) must be taken into account, even for a thin wire.¹

3. NUMERICAL RESULTS

Although no approximations have been introduced in the theoretical basis of this method, when one is dealing with numerical procedures it is necessary to truncate the series in Eq. (18) to a finite number $2N + 1$; i.e.,

$$\sum_{l=-N}^{+N} A_{ml} c_l = b_m \quad (m = -N, \dots, N). \quad (40)$$

With respect to the convergence of Eq. (40), a suggested criterion⁶ based on the properties of the Hankel functions sets $N = ka$. Elsherbeni¹³ and Ragheb and Hamid¹² suggest $N = 3ka$. To verify the validity of these conditions we performed various numerical tests. As an example, in Fig. 3 we show the behavior of the modulus of the expansion coefficients c_l in Eq. (40) for the case of an ideal mirror, for (a) TM and (b) TE polarizations and different values of the truncation index ($N = 1, 3, 9, 15$). The other parameters are $ka = 3$, $kh = 4$, $\varphi = 0^\circ$. As is clearly shown, in both cases the choice $N = 3ka$ seems to be a reasonable compromise between accuracy and computational heaviness.

The second approximation is related to the numerical evaluation of the RW_l functions. Indeed, since in many practical cases, such as dielectric or vacuum-plasma interfaces,³⁰ the expression of the reflection coefficient $\Gamma(n_{||})$ does not allow an analytic evaluation of the integrals in Eq. (10), they must be solved numerically. The evaluation of these integrals has previously been carried out with the use of Gaussian integration techniques.³⁹

The divergences for $|n_{||}| = 1$ were removed by a suitable change of the integration variable. The results obtained in this way are quite satisfactory, as we shall see in the following.

A. Near Field

In Fig. 4 we show two-dimensional (2-D) plots of the modulus of the total electric field E_{tot} on the x - z plane, when the reflecting surface (bottom of each plot) is the interface between the vacuum and an isotropic dielectric medium, and the incident plane wave impinges on it normally ($\varphi = 0^\circ$) from above. On the right-hand side of the figure, schematic drawings of the geometrical arrangement are sketched. The values of the field are codified through a gray scale ranging from black ($E_{\text{tot}} = 0$) to white (maximum of E_{tot}). The plots refer to different choices of the radius of the cylinder [$ka = \pi$, Figs. 4(a) and 4(b); $ka = \pi/10$, Figs. 4(c) and 4(d)], of the cylinder-interface distance [$kh = 3\pi$, Figs. 4(a) and 4(c); $kh = 7\pi/2$, Figs. 4(b) and 4(d)], and of the refractive index of the dielectric medium ($n = 1.1, 2, 50$). The incident wave is TM polarized, so that the E_{tot} vector is parallel to the surface of the cylinder and vanishes there.

We chose the two distances in such a way that the cylinder axis is located in correspondence to antinodal ($kh = 7\pi/2$) and nodal ($kh = 3\pi$) positions of the standing-wave pattern produced by the incident wave impinging on a perfect mirror. We did this to highlight the different perturbations induced by the position of the cylinder.

The three values of the refractive index correspond to

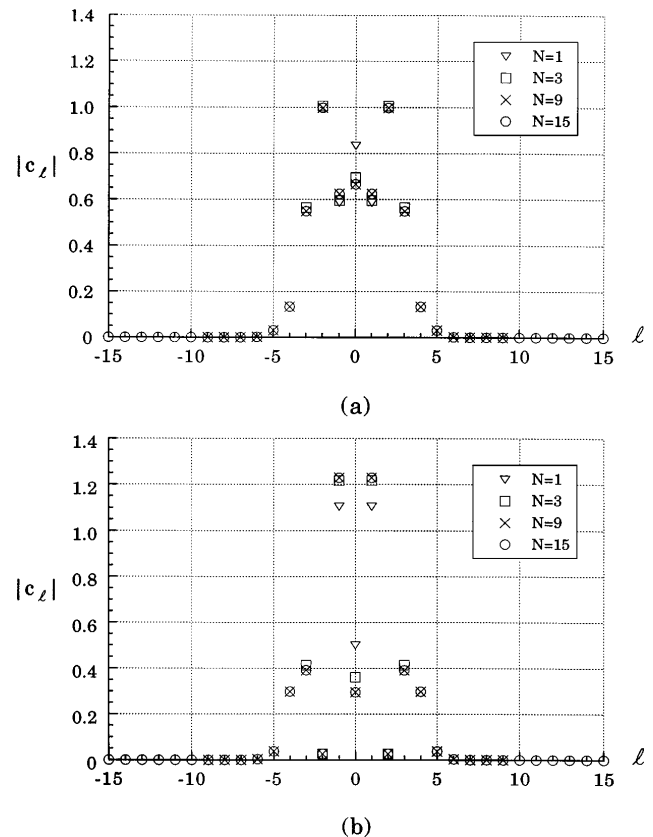


Fig. 3. Behavior of the modulus of expansion coefficients c_l for a dielectric interface ($n = 50$), for (a) TM and (b) TE polarization and different values of the truncation index ($N = 1, 3, 9, 15$). The other parameters are $ka = 3$, $kh = 4$, $\varphi = 0^\circ$.

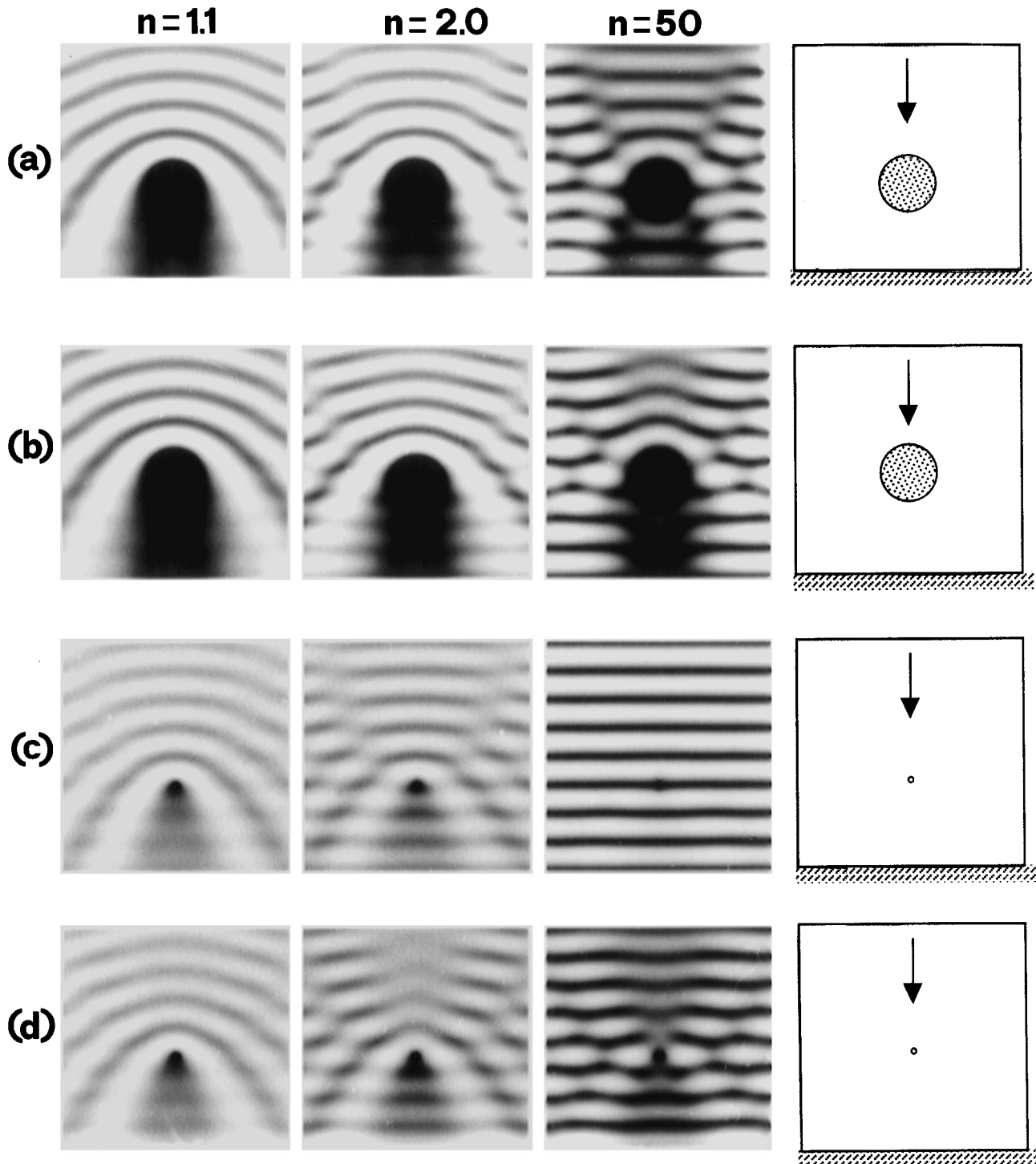


Fig. 4. 2-D plots of the modulus of the E field, for TM polarization: (a) $ka = \pi$, $kh = 3\pi$; $n = 1.1, 2, 50$; (b) $ka = \pi$, $kh = 3.5\pi$; $n = 1.1, 2, 50$; (c) $ka = \pi/10$, $kh = 3\pi$; $n = 1.1, 2, 50$; (d) $ka = \pi/10$, $kh = 3.5\pi$; $n = 1.1, 2, 50$. On the right-hand side, schematic drawings of the geometrical arrangement are sketched. The arrows indicate the direction of the incident plane wave.

a weak ($n = 1.1$), an appreciable ($n = 2$), and a strong ($n = 50$) reflection. The first and the third case may be useful in a comparison with the results for the cases of the absence of any interface and of the presence of an ideal mirror, respectively.¹

Figure 5 shows 2-D plots of the total electric [Fig. 5(a)] and magnetic [Fig. 5(b)] fields when the cylinder is illuminated by a plane TE-polarized wave that

propagates normally to the vacuum-dielectric interface. On the right-hand side of the figure is a schematic drawing of the geometrical arrangement. The radius of the cylinder is $ka = \pi/2$, the refractive index is $n = 2$, and the cylinder-interface distance is $kh = 3\pi$. The evaluation of the electric field for TE polarization, carried out by means of Eq. (27), is an important task, especially in some applications.³⁰

B. Far Field

As highlighted in Section 2, once the expansion coefficients c_l are known, the present method leads to the evaluation of the far field in a simple way by means of relation (38). As an example, in Fig. 6 we show the scattering cross sections¹ when the reflecting surface is the interface between vacuum and a lossless dielectric, for TM (dashed curves) and TE (solid curves) polarizations. Although $ka = \pi$ and $kh = 2\pi$ are kept fixed in all figures,

different φ and refractive index values have been considered ($\varphi = 0^\circ, 30^\circ$; $n = 1.1, 2, 50$).

With a suitable choice of the parameters, the predictions of our procedure can be compared directly with the results obtained by other authors for particular cases. For example, in Ref. 15 the scattering of a Gaussian beam by a perfectly conducting cylinder placed onto a finite conducting plane is carried out. The authors used the extinction theorem⁴⁰ for the evaluation of the far-field

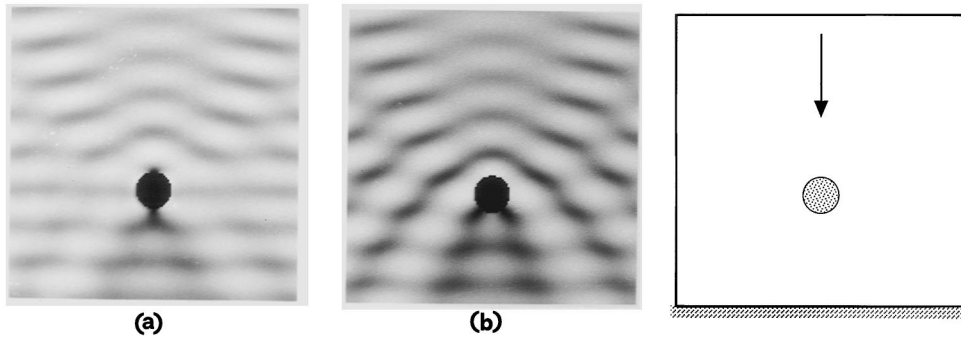


Fig. 5. 2-D plot of the modulus of the (a) H and (b) E fields for TE polarization: $ka = \pi/2, kh = 3\pi, n = 2$. On the right-hand side, a schematic drawing of the geometrical arrangement is sketched. The arrow indicates the direction of the incident plane wave.

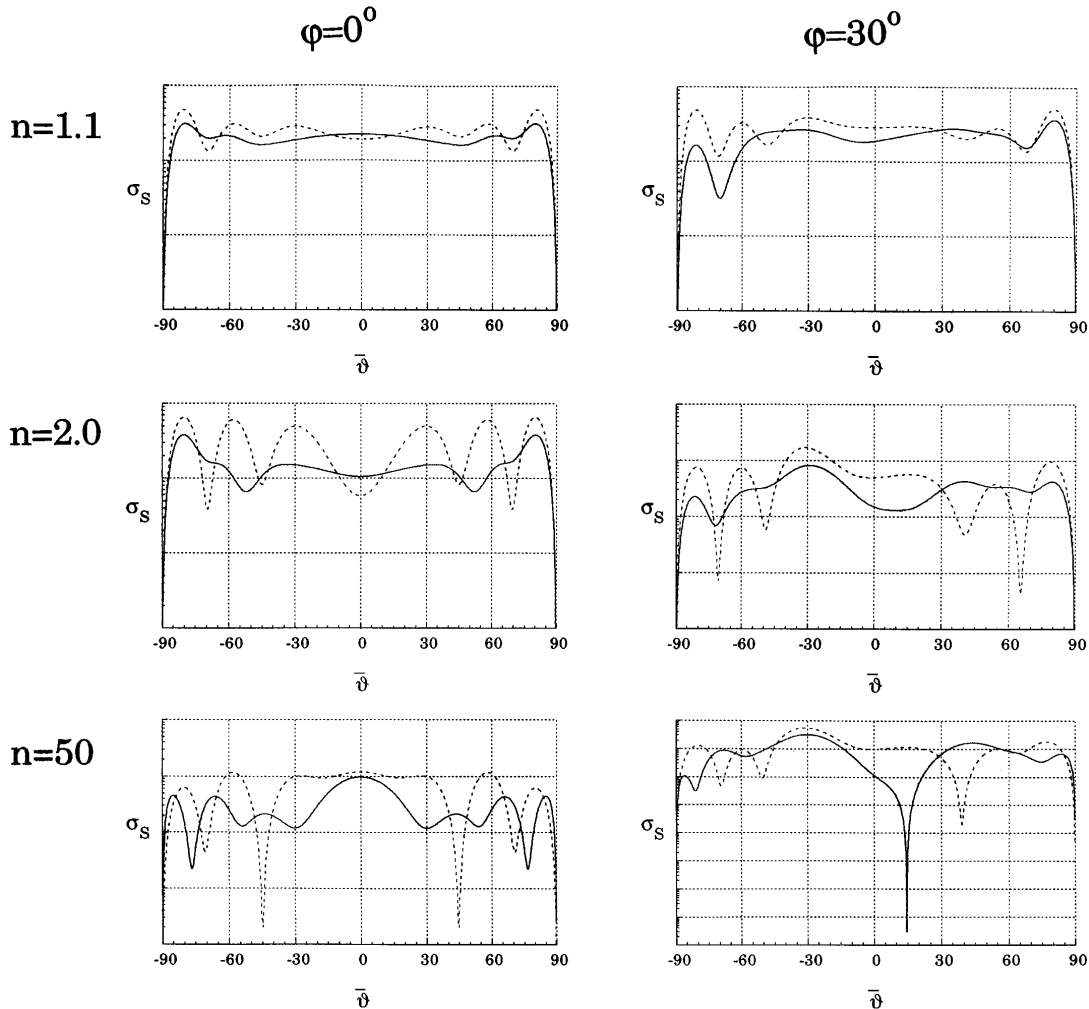


Fig. 6. Semilogarithmic plots (a.u.) of the scattering cross section σ_S as a function of the scattering angle $\bar{\vartheta}$ for the case of a dielectric interface: $ka = \pi, kh = 2\pi, \varphi = 0^\circ, 30^\circ$, and $n = 1.1, 2, 50$, for TE (solid curves) and TM (dashed curves) polarization.

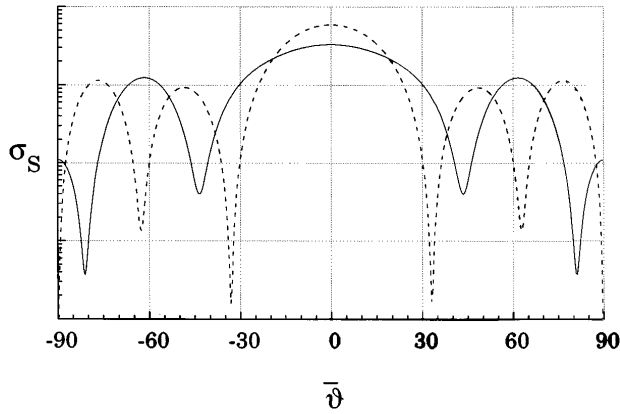


Fig. 7. Semilogarithmic plot (a.u.) of the scattering cross section σ_S as a function of the scattering angle $\bar{\vartheta}$ for an ideal mirror: $ka = kh = 4$, $\varphi = 0^\circ$, for TE (solid curve) and TM (dashed curve) polarization.

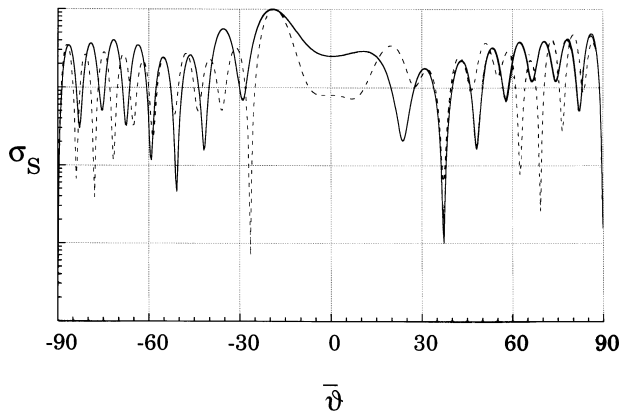


Fig. 8. Semilogarithmic plot (a.u.) of the scattering cross section σ_S as a function of the scattering angle $\bar{\vartheta}$ for a dielectric lossy medium and TM polarization: $n = \sqrt{4.0 + i0.18}$, $kh = 20.94$, $\varphi = 20^\circ$, $ka = 4.19$ (solid curve), $ka = 10.47$ (dashed curve).

pattern. Our results are in perfect agreement with the ones reported in that reference when the spot size of the incident Gaussian beam is much larger than the cylinder size. As an example, in Fig. 7 we show the scattering cross section σ_S as a function of the scattering angle $\bar{\vartheta}$ when $ka = kh = 4$ and $\varphi = 0^\circ$, in both TM (dashed curve) and TE (solid curve) polarization. These curves can be compared with those in Fig. 10 of Ref. 15. The results are identical except for the presence, in the latter case, of a central peak that is due to the reflection of the incident Gaussian beam by the surface (V_r), which is not reported in our figures.

Cottis and Kanellopoulos¹⁸ studied the scattering of a TM-polarized plane wave by a perfectly conducting cylinder near a lossy dielectric interface, by using an integral equation technique for the evaluation of the current distribution on the surface of the cylinder. The results obtained with our method, when $kh = 20.94$, $ka = 4.19$ (solid curve), $ka = 10.47$ (dashed curve), $n = \sqrt{4.0 + i0.18}$, are reported in Fig. 8, which can be compared with Fig. 2 of Ref. 18, for which the same parameters have been used. There is a good qualitative agreement, although the two figures show some differences.

4. CONCLUSIONS

The method presented here gives the solution of plane-wave scattering by a circular, perfectly conducting cylinder of arbitrary radius at a given distance from an arbitrary plane interface. Both the near and the far fields can be accurately determined.

The method seems to be simple and general and can be applied to any plane surfaces, such as dielectric interfaces, multilayered structures, and anisotropic and lossy media. A further attractive feature is that both polarization states can be treated with essentially the same procedure.

The problem of scattering by an array of arbitrarily placed circular cylinders (either conducting or dielectric) with parallel axes has been treated by several authors using different techniques^{13,14} for a homogeneous medium. Our method may be generalized to treat such a problem in the presence of a plane interface. Therefore it should prove useful in a variety of practical applications, both in optics and in microwaves.

Furthermore, by means of a suitable plane-wave decomposition, our method can be extended to more complicated incident fields, such as Gaussian beams.

APPENDIX A

Let us consider a general field distribution $V_i(\xi, \zeta)$ (with $\xi < 0$) impinging on a surface coinciding with the $\xi = \chi$ plane and characterized by the reflection coefficient $\Gamma(n_{\parallel})$. Our aim is to study the field reflected by the surface. By means of a plane-wave expansion of the field $V_i(\xi, \zeta)$ on the $\xi = 0$ plane, we get

$$V_i(0, \zeta) = \frac{1}{2\pi} \int_{-\infty}^{+\infty} A_i(0, n_{\parallel}) \exp(in_{\parallel}\zeta) dn_{\parallel}, \quad (\text{A1})$$

where the function $A_i(\xi, n_{\parallel})$ is the angular spectrum of the field in a plane $\xi = \text{constant}$.

The field on the surface $\xi = \chi$ can be expressed in terms of $A_i(0, n_{\parallel})$ by consideration of the propagation features of the angular spectrum; i.e.,

$$\begin{aligned} V_i(\chi, \zeta) &= \frac{1}{2\pi} \int_{-\infty}^{+\infty} A_i(\chi, n_{\parallel}) \exp(in_{\parallel}\zeta) dn_{\parallel} \\ &= \frac{1}{2\pi} \int_{-\infty}^{+\infty} A_i(0, n_{\parallel}) \exp(in_{\perp}\chi + in_{\parallel}\zeta) dn_{\parallel}. \end{aligned} \quad (\text{A2})$$

The angular spectrum of the reflected field can be simply expressed by means of the definition of the reflection coefficient; i.e.,

$$A_r(\chi, n_{\parallel}) = A_i(\chi, n_{\parallel}) \Gamma(n_{\parallel}) = A_i(0, n_{\parallel}) \exp(in_{\perp}\chi) \Gamma(n_{\parallel}). \quad (\text{A3})$$

Thus we have

$$\begin{aligned} V_r(\chi, \zeta) &= \frac{1}{2\pi} \int_{-\infty}^{+\infty} A_r(\chi, n_{\parallel}) \exp(in_{\parallel}\zeta) dn_{\parallel} \\ &= \frac{1}{2\pi} \int_{-\infty}^{+\infty} A_i(0, n_{\parallel}) \Gamma(n_{\parallel}) \exp(in_{\perp}\chi + in_{\parallel}\zeta) dn_{\parallel}. \end{aligned} \quad (\text{A4})$$

The reflected field on a plane $\xi = \text{constant} < \chi$ is

$$V_r(\xi, \zeta) = \frac{1}{2\pi} \int_{-\infty}^{+\infty} A_i(0, n_{\parallel}) \Gamma(n_{\parallel}) \exp(in_{\perp}\chi) \\ \times \exp[in_{\perp}(\chi - \xi) + in_{\parallel}\zeta] dn_{\parallel} \quad (\text{A5})$$

$$= \frac{1}{2\pi} \int_{-\infty}^{+\infty} A_i(0, n_{\parallel}) \Gamma(n_{\parallel}) \\ \times \exp[in_{\perp}(2\chi - \xi) + in_{\parallel}\zeta] dn_{\parallel}, \quad (\text{A6})$$

where the backward propagation of the reflected plane waves has been taken into account. Now Eq. (A5) can be written, using the convolution theorem for Fourier transform, as

$$V_r(\xi, \zeta) = V_i(2\chi - \xi, \zeta) * \hat{\Gamma}(\zeta), \quad (\text{A7})$$

where the asterisk denotes convolution with respect to the ζ variable and $\hat{\Gamma}(\zeta)$ is the inverse Fourier transform of the reflection coefficient; i.e.,

$$\hat{\Gamma}(\zeta) = \frac{1}{2\pi} \int_{-\infty}^{+\infty} \Gamma(n_{\parallel}) \exp(in_{\parallel}\zeta) dn_{\parallel}. \quad (\text{A8})$$

Equation (A7), applied to the fields V_d and V_{dr} , coincides with Eq. (6) of Section 2.

APPENDIX B

Starting from Eq. (11) of Ref. 34, and referring to Fig. 1 of the same reference, we have

$$H_l(\rho) \exp(il\vartheta) = \int_{-\infty}^{+\infty} F'_l(\eta, \beta) \exp(i\beta\xi) d\beta, \quad (\text{B1})$$

where in this case the prime is used to distinguish the old notation from the present one. The two sets of functions are different because a new frame of reference is now employed. Explicit expression of the above-mentioned F'_l functions is given in Eq. (12) of Ref. 34. Our purpose is to obtain the expression of the F_l functions used throughout the paper, which are defined as

$$H_l(\rho) \exp(il\vartheta) = \frac{1}{2\pi} \int_{-\infty}^{+\infty} F_l(\xi, n_{\parallel}) \exp(in_{\parallel}\zeta) dn_{\parallel}. \quad (\text{B2})$$

To this end, it is necessary to change the frame of reference. This requires the following substitutions:

$$\alpha \rightarrow \pi/2 - \vartheta, \quad \xi \rightarrow \zeta, \quad \eta \rightarrow \xi, \quad \beta \rightarrow n_{\parallel}. \quad (\text{B3})$$

After the substitutions we obtain

$$i^l H_l(\rho) \exp(-il\vartheta) = \int_{-\infty}^{+\infty} F'_l(\xi, n_{\parallel}) \exp(in_{\parallel}\zeta) dn_{\parallel}. \quad (\text{B4})$$

By changing l to $-l$ and using the well-known property $H_{-l}(\rho) = (-1)^l H_l(\rho)$, we have

$$i^{-l} (-1)^l H_l(\rho) \exp(il\vartheta) = \int_{-\infty}^{+\infty} F'_l(\xi, n_{\parallel}) \exp(in_{\parallel}\zeta) dn_{\parallel}, \quad (\text{B5})$$

and therefore

$$H_l(\rho) \exp(il\vartheta) = \int_{-\infty}^{+\infty} (-i)^l F'_{-l}(\xi, n_{\parallel}) \exp(in_{\parallel}\zeta) dn_{\parallel}. \quad (\text{B6})$$

By comparing Eq. (B2) with Eq. (B6), we obtain the following expression:

$$F_l(\xi, n_{\parallel}) = 2\pi (-i)^l F'_{-l}(\xi, n_{\parallel}). \quad (\text{B7})$$

By recalling Eq. (12) of Ref. 34 we finally obtain

$$F_l(\xi, n_{\parallel}) = \begin{cases} (-1)^l \frac{2 \exp\left(-\xi \sqrt{n_{\parallel}^2 - 1}\right)}{i \sqrt{n_{\parallel}^2 - 1}} \left(\sqrt{n_{\parallel}^2 - 1} - n_{\parallel}\right)^{-l} & \text{for } n_{\parallel} \in (-\infty, -1) \\ \frac{2 \exp\left(i\xi \sqrt{1 - n_{\parallel}^2} - il \arccos n_{\parallel}\right)}{\sqrt{1 - n_{\parallel}^2}} & \text{for } n_{\parallel} \in (-1, 1) \\ \frac{2 \exp\left(-\xi \sqrt{n_{\parallel}^2 - 1}\right)}{i \sqrt{n_{\parallel}^2 - 1}} \left(\sqrt{n_{\parallel}^2 - 1} + n_{\parallel}\right)^l & \text{for } n_{\parallel} \in (1, +\infty) \end{cases}. \quad (\text{B8})$$

Taking into account the algebraic relation

$$(-1)^l \left(\sqrt{n_{\parallel}^2 - 1} - n_{\parallel}\right)^{-l} = \left(\sqrt{n_{\parallel}^2 - 1} + n_{\parallel}\right)^l, \quad (\text{B9})$$

we can rewrite Eq. (B8) as

$$F_l(\xi, n_{\parallel}) = \frac{2 \exp\left(i\xi \sqrt{1 - n_{\parallel}^2}\right)}{\sqrt{1 - n_{\parallel}^2}} g_l(n_{\parallel}), \quad (\text{B10})$$

where $g_l(n_{\parallel})$ is defined as

$$g_l(n_{\parallel}) = \begin{cases} \left(\sqrt{n_{\parallel}^2 - 1} + n_{\parallel}\right)^l & \text{for } |n_{\parallel}| \geq 1 \\ \exp(-il \arccos n_{\parallel}) & \text{for } |n_{\parallel}| \leq 1 \end{cases}. \quad (\text{B11})$$

In particular, Eqs. (B11) can be formally rewritten in a compact form by use of the definition of the arccos function in the complex domain.⁴¹ Finally, after some algebra, we can write

$$F_l(\xi, n_{\parallel}) = \frac{2 \exp\left(i\xi \sqrt{1 - n_{\parallel}^2} - il \arccos n_{\parallel}\right)}{\sqrt{1 - n_{\parallel}^2}} \quad \text{for } n_{\parallel} \in (-\infty, +\infty), \quad (\text{B12})$$

which coincides with Eq. (11) of Section 2.

APPENDIX C

We start from the definition of the function $RW_m(\xi, \zeta)$:

$$RW_m(\xi, \zeta) = \frac{1}{2\pi} \int_{-\infty}^{+\infty} \Gamma(n_{\parallel}) F_m(\xi, n_{\parallel}) \exp(in_{\parallel}\zeta) dn_{\parallel}. \quad (C1)$$

In particular, for the case $\Gamma(n_{\parallel}) = 1$, we have $RW_m(\xi, \zeta) = CW_m(\xi, \zeta)$. By recalling Eq. (11), we obtain from Eq. (C1)

$$\begin{aligned} RW_{m+1}(\xi, \zeta) &= \frac{1}{2\pi} \int_{-\infty}^{+\infty} \Gamma(n_{\parallel}) \frac{2 \exp(i\xi n_{\perp})}{n_{\perp}} \\ &\quad \times \exp[-i(m+1)\arccos n_{\parallel}] \exp(i\zeta n_{\parallel}) dn_{\parallel} \\ &= \frac{1}{2\pi} \int_{-\infty}^{+\infty} \Gamma(n_{\parallel}) F_m(\xi, n_{\parallel}) \exp(-i \arccos n_{\parallel}) \\ &\quad \times \exp(in_{\parallel}\zeta) dn_{\parallel}. \end{aligned} \quad (C2)$$

We take into account the trigonometric relation

$$\begin{aligned} \exp(-i \arccos n_{\parallel}) &= \cos(\arccos n_{\parallel}) - i \sin(\arccos n_{\parallel}) \\ &= n_{\parallel} - in_{\perp}, \end{aligned} \quad (C3)$$

and Eq. (C2) becomes

$$\begin{aligned} RW_{m+1}(\xi, \zeta) &= \frac{1}{2\pi} \int_{-\infty}^{+\infty} \Gamma(n_{\parallel}) F_m(\xi, n_{\parallel}) (n_{\parallel} - in_{\perp}) \exp(in_{\parallel}\zeta) dn_{\parallel} \\ &= \frac{1}{2\pi} \int_{-\infty}^{+\infty} n_{\parallel} \Gamma(n_{\parallel}) F_m(\xi, n_{\parallel}) \exp(in_{\parallel}\zeta) dn_{\parallel} \\ &\quad - \frac{1}{2\pi} \int_{-\infty}^{+\infty} in_{\perp} \Gamma(n_{\parallel}) F_m(\xi, n_{\parallel}) \exp(in_{\parallel}\zeta) dn_{\parallel} \\ &= -i\partial_{\zeta} RW_m(\xi, \zeta) - \partial_{\xi} RW_m(\xi, \zeta). \end{aligned} \quad (C4)$$

Proceeding in the same way for RW_{m-1} , we get the following linear system:

$$\begin{aligned} RW_{m+1}(\xi, \zeta) &= -i\partial_{\zeta} RW_m(\xi, \zeta) - \partial_{\xi} RW_m(\xi, \zeta), \\ RW_{m-1}(\xi, \zeta) &= -i\partial_{\zeta} RW_m(\xi, \zeta) + \partial_{\xi} RW_m(\xi, \zeta), \end{aligned} \quad (C5)$$

and, by inversion, finally we obtain

$$\partial_{\xi} RW_m(\xi, \zeta) = 1/2[RW_{m-1}(\xi, \zeta) - RW_{m+1}(\xi, \zeta)], \quad (C6)$$

$$\partial_{\zeta} RW_m(\xi, \zeta) = i/2[RW_{m-1}(\xi, \zeta) + RW_{m+1}(\xi, \zeta)]. \quad (C7)$$

Equations (C6) and (C7) coincide with Eqs. (30) and (31), respectively. Equations (28) and (29) can be simply derived by replacement of RW with CW in Eqs. (C6) and (C7), respectively.

ACKNOWLEDGMENTS

We thank the anonymous referees for their useful comments and suggestions. This research is supported in part by Istituto Nazionale di Fisica della Materia and Ministero dell' Università e della Ricerca Scientifica e Tecnologica.

REFERENCES

1. J. J. Bowman, T. B. Senior, and P. L. E. Uslenghi, *Electromagnetic and Acoustic Scattering by Simple Shapes* (Hemisphere, New York, 1987); J. T. Ruck, D. E. Barrick, W. D. Stuart, and C. K. Krichbaum, *Radar Cross Section Handbook* (Plenum, New York, 1970).
2. A. Ishimaru, *Electromagnetic Wave Propagation, Radiation and Scattering* (Prentice-Hall, Englewood Cliffs, N.J., 1991), Chap. 11.
3. J. H. Richmond, "Scattering by an arbitrary array of parallel wires," *IEEE Trans. Microwave Theory Tech.* **MTT-13**, 408–412 (1965).
4. C. R. Mullin, R. Sandburg, and C. O. Velline, "A numerical technique for the determination of scattering cross sections of infinite cylinders of arbitrary cross section," *IEEE Trans. Antennas Propag.* **AP-13**, 141–149 (1965).
5. W. A. Imbriale and R. Mittra, "The two-dimensional inverse scattering problem," *IEEE Trans. Antennas Propag.* **AP-18**, 633–642 (1970).
6. D. R. Wilton and R. Mittra, "A new numerical approach to the calculation of electromagnetic scattering properties of two-dimensional bodies of arbitrary cross section," *IEEE Trans. Antennas Propag.* **AP-20**, 310–317 (1972).
7. F. Zolla, R. Petit, and M. Cadilhac, "Electromagnetic theory of diffraction by a system of parallel rods: the method of fictitious sources," *J. Opt. Soc. Am. A* **11**, 1087–1096 (1994).
8. J. R. Wait, "Reflection from a wire grid parallel to a conducting plane," *Can. J. Phys.* **32**, 571–579 (1954).
9. T. C. Rao and R. Barakat, "Plane-wave scattering by a conducting cylinder partially buried in a ground plane. 1. TM case," *J. Opt. Soc. Am. A* **6**, 1270–1280 (1989).
10. T. C. Rao and R. Barakat, "Plane-wave scattering by a conducting cylinder partially buried in a ground plane. 2. TE case," *J. Opt. Soc. Am. A* **8**, 1986–1990 (1991).
11. T. C. Rao and R. Barakat, "Near field scattering by a conducting cylinder partially buried in a conducting plane," *Opt. Commun.* **111**, 18–25 (1994).
12. H. A. Ragheb and M. Hamid, "Scattering by N parallel conducting circular cylinders," *Int. J. Electron.* **59**, 407–421 (1985).
13. A. Z. Elsherbeni, "A comparative study of two-dimensional multiple scattering techniques," *Radio Sci.* **29**, 1023–1033 (1994).
14. D. Felbacq, G. Tayreb, and D. Maystre, "Scattering by a random set of parallel cylinders," *J. Opt. Soc. Am. A* **11**, 2526–2538 (1994).
15. P. J. Valle, F. González, and F. Moreno, "Electromagnetic wave scattering from conducting cylindrical structures on flat substrates: study by means of the extinction theorem," *Appl. Opt.* **33**, 512–523 (1994).
16. P. J. Valle, F. Moreno, J. M. Saiz, and F. González, "Near-field scattering from subwavelength metallic protuberances on conducting flat substrates," *Phys. Rev. B* **51**, 13681–13690 (1995).
17. A. Madrazo and M. Nieto-Vesperinas, "Scattering of electromagnetic waves from a cylinder in front of a conducting plane," *J. Opt. Soc. Am. A* **12**, 1298–1309 (1995).
18. P. G. Cottis and J. D. Kanellopoulos, "Scattering from a conducting cylinder above a lossy medium," *Int. J. Electron.* **65**, 1031–1038 (1988).
19. M. A. Taubenblatt, "Light scattering from cylindrical structures on surfaces," *Opt. Lett.* **15**, 255–257 (1990).
20. P. A. Bobbert and J. Vlieger, "Light scattering by a sphere on a substrate," *Physica* **137A**, 209–242 (1986).
21. K. B. Nahm and W. L. Wolfe, "Light scattering for spheres on a conducting plane: comparison with experiment," *Appl. Opt.* **26**, 2995–2999 (1987).
22. G. Videen, "Light scattering from a sphere on or near a surface," *J. Opt. Soc. Am. A* **8**, 483–489 (1991).
23. G. Videen, M. G. Turner, V. J. Iafelice, W. S. Bickel, and W. L. Wolfe, "Scattering from a small sphere near a surface," *J. Opt. Soc. Am. A* **10**, 118–126 (1993).
24. B. R. Johnson, "Light scattering from a spherical particle on a conducting plane: I. Normal incidence," *J. Opt. Soc. Am. A* **9**, 1341–1351 (1992).

25. I. V. Lindell, A. H. Sihlova, K. O. Muinonen, and P. W. Barber, "Scattering by a small object close to an interface. I. Exact-image theory formulation," *J. Opt. Soc. Am. A* **8**, 472–476 (1991).
26. M. A. Taubenblatt and T. K. Tran, "Calculation of light scattering from particles and structures on a surface by the coupled-dipole method," *J. Opt. Soc. Am. A* **10**, 912–919 (1993).
27. F. Moreno, F. González, J. M. Saiz, P. J. Valle, and D. L. Jordan, "Experimental study of copolarized light scattering by spherical metallic particles on conducting flat substrates," *J. Opt. Soc. Am. A* **10**, 141–157 (1993).
28. J. R. Wait, "The impedance of a wire grid parallel to a dielectric interface," *IRE Trans. Microwave Theory Tech.* **5**, 99–102 (1957).
29. J. R. Wait, "Note on solution for scattering from parallel wires in an interface," *J. Electromagn. Waves Appl.* **4**, 1151–1155 (1990).
30. F. Frezza, F. Gori, M. Santarsiero, F. Santini, and G. Schettini, "Quasi-optical launchers for lower hybrid waves: a full-wave approach," *Nucl. Fusion* **34**, 1239–1246 (1994).
31. J. R. Wait, *Electromagnetic Radiation from Cylindrical Structures* (Peter Peregrinus, London, 1988).
32. R. Petit, ed., *Electromagnetic Theory of Gratings* (Springer-Verlag, Berlin, 1980).
33. A. J. Pidduck, D. J. Robbins, I. M. Young, A. G. Cullis, and A. R. S. Martin, "The formation of dislocations and their *in-situ* detection during silicon vapor phase epitaxy at reduced temperature," *Mater. Sci. Eng. B* **4**, 417–422 (1989).
34. G. Cincotti, F. Gori, M. Santarsiero, F. Frezza, F. Furnò, and G. Schettini, "Plane wave expansion of cylindrical functions," *Opt. Commun.* **95**, 192–198 (1993).
35. M. Abramowitz and I. Stegun, *Handbook of Mathematical Functions* (Dover, New York, 1972).
36. J. R. Wait, *Electromagnetic Wave Theory* (Harper & Row, New York, 1985).
37. W. Wang, R. Simon, and E. Wolf, "Changes in the coherence and spectral properties of partially coherent light reflected from a dielectric slab," *J. Opt. Soc. Am. A* **9**, 287–297 (1992).
38. Ref. 36, Sec. 4.15.
39. W. H. Press, S. A. Teukolsky, W. T. Vetterling, and B. P. Flannery, *Numerical Recipes in FORTRAN—The Art of Scientific Computing*, 2nd ed. (Cambridge U. Press, Cambridge, 1992).
40. E. Wolf, "A generalized extinction theorem and its rule in scattering theory," in *Coherence and Quantum Optics*, L. Mandel and E. Wolf, eds. (Plenum, New York, 1973), pp. 339–357.
41. A. I. Markushevich, *The Theory of Analytic Functions: a Brief Course* (Mir, Moscow, 1983).